

# Enhancing concrete sustainability: a neural networks hybrid optimization approach to predicting compressive strength using supplementary cementitious materials

Esra'a Alhenawi<sup>1</sup>, Ayat Mahmoud Al-Hinawi<sup>2</sup>, Zaher Salah<sup>3</sup>, Omar Alidmat<sup>1</sup>, Esraa Abu Eloud<sup>1</sup>,  
Raed Alazaidah<sup>1</sup>, Bashar Rizik AlSayyed<sup>4</sup>

<sup>1</sup>Department of Computer Science, Faculty of Information Technology, Zarqa University, Zarqa, Jordan

<sup>2</sup>Department of Allied Engineering Sciences, Faculty of Engineering, The Hashemite University, Zarqa, Jordan

<sup>3</sup>Department of Information Technology, Faculty of Prince Al-Hussein Bin Abdullah II for Information Technology,  
The Hashemite University, Zarqa, Jordan

<sup>4</sup>Department of Civil Engineering, Faculty of Engineering, University of Jordan, Amman, Jordan

## Article Info

### Article history:

Received Aug 30, 2024

Revised Jun 19, 2025

Accepted Jun 30, 2025

### Keywords:

Firefly algorithm optimization

Gas emissions

Greenhouse

Supplementary cementitious  
materials

Sustainable construction

## ABSTRACT

This research evaluates the implementation of advanced machine learning methodologies for concrete mix design to achieve better predictive models and sustainable outcomes. This study develops a hybrid optimization approach by combining dung beetle optimizer (DBOA) and firefly algorithm (FLA) to optimize hyperparameters for convolutional-recurrent neural networks in order to correctly predict concrete compressive strength when using supplementary cementitious materials (SCMs). Shapley additive explanations (SHAP) provide feature significance analysis, which ensures that the model produces understandable conclusions supported by empirical findings. The findings demonstrate that this method enhances the predictive accuracy of strength analysis, along with offering critical insights about SCM usage in order to improve sustainable construction methods. The model proves suitable for integration into actual concrete mix design and quality control systems because it achieves both computational speed and passes validation tests on distinct datasets. The research creates foundations for upcoming studies about multimodal learning enrichment and deals with ethical concerns in construction site safety when using machine learning systems.

This is an open access article under the [CC BY-SA](#) license.



## Corresponding Author:

Zaher Salah

Department of Information Technology, Faculty of Prince Al-Hussein Bin Abdullah II for Information  
Technology, The Hashemite University

Zarqa, Jordan

Email: zaher@hu.edu.jo

## 1. INTRODUCTION

The building industry has implemented many cement manufacturing greenhouse gas emission reduction measures [1], [2]. Similar to burning gasoline, the manufacture of hydraulic cement accounts for 7%–9% of world carbon dioxide emissions [3]–[5]. To lower CO<sub>2</sub> emissions, cement mixes can include waste or industrial flows as multi-component binders [3], [6]–[14]. One way to cut greenhouse gas emissions by 47% to 5% is to use industrial waste instead of cement, such as ground granulated blast furnace slag (GGBS) from blast furnace iron ore extraction [15], [16]. One ton of GGBS production has a worldwide environmental emission factor of 0.143 t CO<sub>2</sub>-e/ton, which is less than the standard established by most

nations and international organizations. Cement uses 9 t CO<sub>2</sub>-e/ton, although concrete mixes are made using transportation technologies [17].

About 60% of the 530 million tons of global slag (GGBS) is used in construction [18], [19]. GGBS has been studied on various concrete and mortar types [3], [20], [21]. Another study [22] found that MS and GGBS synergistically improved concrete resistance to unfavorable consequences. According to a different research [23], resistance and durability without PC were best boosted by 20% MBS made from rice husk and by using slag powder instead. By converting fly ash and powdered blast furnace slag, waste glass-derived nano powder, into alkali-activated mortars, drying shrinkage is decreased and wear, freeze-thaw cycles, and sulfuric acid resistance are enhanced [24]. According to other studies, GGBS should be used in place of 20% of cement before sample workability and porosity cause resistance to drop [15], [25].

The workability, bleeding, heat of hydration, corrosion, porosity, and permeability of both fresh and hardened concrete are all improved by GGBS in cement [26]–[29]. Due to greater particle distribution, GGBS improved concrete workability by 40% [3]. Cement paste fills aggregate micro-spaces to reduce internal friction between concrete components, improving workability [25], [30].

Tensile strength, a vital road concrete property, has design parameter constraints that should be controlled to minimize cracks [31]. Concrete shrinkage depends on cement, water, aggregates, air dryness, and rising temperature [32]. Cement dose, C3A content, gel component, and alkali content affect shrinkage [33]. Early setting reduces cement paste volume by 1% of dry cement volume [33], [34].

Shrinking values fall below zero. Concretes with a lot of binder can reach 6 mm/m [35]. Size decreases by 5% after one month, 60% after three months, and 75% after a year [32]. W/C ratios cause concrete pores to expand, which increases shrinkage. Additional aggregates prevent shrinkage because they are coarser [36]. More than 50% relative humidity and 800 ppm CO<sub>2</sub> increase shrinkage rates because CO<sub>2</sub> dissolves and eliminates hydrosilicate hydration products [35]. The carbonation process is accelerated by high external CO<sub>2</sub> concentrations, lowering the pH from 12–13 to less than 9 and rupturing the reinforcing bar's passivation layer, which causes corrosion [37]–[40].

As the largest component of concrete, aggregate usage has the greatest environmental impact. Annual international building aggregate demand exceeds 10 billion tons [41]–[44]. Road asphalt pavement (RAP) aggregates [45]–[47], quarry sand (QS) [48], recycled aggregate concrete (RAC) from building demolitions [43], [44], and ecological mortar that replaces natural aggregates with glass waste [49] have all been the subject of cadaveric research.

ACBFS is another air-cooled road concrete aggregate source [50], [51]. It has been demonstrated that natural aggregates made from blast furnace slag may be used in asphalt [52]. For concrete structures, the Japanese Guide suggests a 20%–60% combination of natural and fine materials [53]. The reference standard for blast furnace slag concrete aggregates in our nation has been SR EN 12620 since 2003 [54]. It is possible to incorporate steel industry waste materials into road concrete mixtures, but it is important to assess how they affect both fresh and hardened concrete [55]. Utilizing innovative technologies and reusing synthetic materials can help the environment by reducing manufacturing costs and conserving non-renewable resources [56].

A low-carbon circular economy is a global goal, and the building industry is promoting green alternatives and minimizing environmental harm caused by the cement industry. The production of concrete and cement produces almost no emissions. Nine metric tons of CO<sub>2</sub> must be released by the cement industry for every metric ton of cement produced. There are major repercussions linked to the global emissions from the building industry. Therefore, one of the greatest approaches to reduce greenhouse gas emissions is to replace cement with similar materials [57]. Supplementary cementitious materials (SCMs) are cost-effective and ecologically beneficial alternatives to cement. Most SCMs are pozzolanic, which improve concrete microstructure, late strength, and CO<sub>2</sub> emissions [58].

Fly ash (FA) from coal power stations is the most common SCM in cement-based materials. Industry standards recommend replacing cement with FA by 10%–30% [59], [60]. High volume fly ash (HVFA) concrete has the best mechanical properties and durability, making it a sustainable construction material [61]–[66]. Following 56 and 91 days of mixing FA with cement and replacing 50% of the cement with FA at a W/C ratio of 0.42, Bouzoubaâ *et al.* [67] achieved compressive strengths of 32.2 MPa and 35.2 MPa. These values were greater than ordinary portland cement (OPC) concrete's 0.53. According to Mardani-Aghabbaglou and Ramyar [68], after 180 days, 60% FA replacement increased compressor strength by 15%–18% above OPC. According to Chen *et al.* [69], drying shrinkage was decreased by 23%–30% when FA was substituted for 50%–80% of the cement. According to Müllauer *et al.* [70], 70% FA successfully decreased alkali-aggregate reactions. According to Wang *et al.* [71], to reduce the porosity of concrete, 30% by weight of coarse aggregate should be used for FGPS and 15% for FA. Additionally, Wang *et al.* [72] discovered that adding 30% FA to panel concrete improved its permeability and compressive strength with time.

Granulated ground blast furnace slag (GGBFS) blast furnace iron waste is frequently used as a cement alternative. Glassy blast furnace slag is quenched and cooled to form GGBFS, which binds well. Crossin [16] found that GGBFS as an SCM reduced greenhouse gas transparency by 47.5%. After 28 days of curing, the mechanical strength of ternary mixed cement containing a larger percentage of GGBFS was greater than that of OPC [22], [73], [74]. Due to the diluting effect, Lim *et al.* [75] discovered that ternary mixed cement containing GGBFS had a lower peak compressive strength than OPC. However, it did better than

After 28 to 365 days of therapy, OPC and acquired more between 28 and 91 days [73]–[77]. Cheah *et al.* [78] investigated a ternary mixed cement mortar that contained cement, GGBFS, and ground coal bottom ash (GCBA). They discovered that the mechanical and physical characteristics of cement mortar were enhanced by 40% GGBFS and 5% GCBA without SP and 40% GGBFS and 10% GCBA with SP [79].

Research on waste concrete aggregates and ternary cementitious ingredients like silica fume and GGBFS revealed that adding GGBFS to 25% of cement increased the GW P value. According to Weise *et al.* [80], the 30% weight metakaolin mix consumed the most CH between days 28 and 56, which had an impact on strength. Using SCMs in concrete improves cement reaction, but metakaolin content increases efficiency [81]. SCMs like FA and GGBFS can enable a low-carbon circular economy in building. These materials reduce greenhouse gas emissions and increase concrete structure efficiency and duration, encouraging construction sustainability.

Impermeability in concrete affects resistance to water-soluble chloride ions, CO<sub>2</sub>, and sulfate, which impair concrete durability. These chemicals can infiltrate concrete, degrade it, and limit its lifespan, making them global threats [82]–[84]. Concrete porosity, which affects its permeability, depends on its size, shape, and interfacial transition zone. Recycled fine aggregate (RFA) %, W/C ratio, and mineral admixtures directly affect recycled fine aggregate concrete (RFAC) impermeability. According to research, admixtures and additives optimize concrete's microscopic structure, boosting its impermeability [85]–[87].

Concrete porosity is highly dependent on RFA quantitative properties. RFA has fewer physical properties than natural fine aggregates. Because RFAC uses more RFA, its performance is usually poorer. RFA particles absorb gaps and microcracks from the previous mortar because of their poor grading, which makes the concrete porous. Thus, RFAC replacement increases the water vapor transmission barrier [88]–[91]. Because RFA is porous and absorbs water, SCC mixtures absorb more water with a higher RFA substitution rate. However, RFAC's permeability is lower in a sulfate environment than in regular concrete, and its water absorption is 25% lower [92]. The W/C ratio is crucial to concrete preparation and permeability resistance. A W/C ratio of 0.65 reduces impermeability compared to 0.55. Because a larger W/C ratio slows RFAC cement hydration, pores form and concrete compactness decreases [88], [89], [93].

FA can replace silicate cement in construction due to its pozzolanic characteristics [93]. Concrete that contains fine fly ash has better hydration, zeolite, accumulation, and nucleation [94]. Concrete density rises as a result of the early hydration response of FA, which increases the quantity of hydration products in the pores [95]. The permeability of self-compacting concrete containing 10% FA and 100% RFA was lower than that of control mixes devoid of FA [96].

Due to RFA's poor physical and chemical characterization and RAC's weak interfacial transition zone (ITZ), alternative mixing strategies have been introduced. This comprises the optimal triple mixing technique (OTM), triple mixing method (TM) [97], and double mixing method (DM) [98]. To conclude, OTM staff add SPs, water-reducing agents, in varied orders. SP is added to the mix with other gelling components to increase gelling and ITZ proportion. This method uses the zeolite effect more effectively; hence the RAC has an 8-permeability rating [99]. By choosing the correct materials and ratios and improving procedures, the building industry can waterproof and strengthen concrete. This provides durable constructions. RFA beats NFA due to fine aggregate's poor water absorption. RFA's water content must be evaluated before integration because higher absorption affects concrete's mechanical qualities. AD, OD, and SSD RFA methods were tested for RFAC permeability. The study found that RFA permeability resistance in concrete follows the order SSD > AD > OD, while for recycled coarse aggregate, the order is reversed (SSD < AD < OD) [100]. Compared to RCA, RFA restricts water more because its particles are smaller and its specific surface area is larger [101]. Concrete pore size is significantly impacted by RFA integration, and permeability is decreased by raising the W/C ratio and RFA replacement rate, as shown in Figure 1.

Saturated surface-dried RFA, improved mixing, and fly ash addition, on the other hand, consistently lower RFAC permeability. Fly ash with two pozzolanic minerals, silica fume, and metakaolin, together, increases the impermeability of RFAC. Table 1 lists the variables influencing RFAC sealing. In conclusion, although increased water absorption is a problem with RFA, its permeability and durability may be significantly increased by controlling its moisture content, merging SCM, and using the precise mix proportions for RFAC.

This paper presents a unique hybrid optimization technique that combines the dung beetle optimizer (DBOA) and firefly algorithm (FLA) to improve the hyperparameters of a convolutional-recurrent neural

network in addition to using traditional approaches. Through their combination, the approach performs a strong global search using FLA alongside precise local search optimization done by DBOA. Our method combines conceptual novelty by applying biological concepts to material scientific applications when predicting concrete compressive strength as an essential factor for sustainable construction. In addition, this research aims to address the critical gap in sustainable construction practices by significantly reducing the CO<sub>2</sub> emissions associated with conventional cement production. The study examines how concrete's mechanical characteristics change after supplemental cementitious materials (SCMs) such fly ash (FA) and ground granulated blast furnace slag (GGBS) are added.

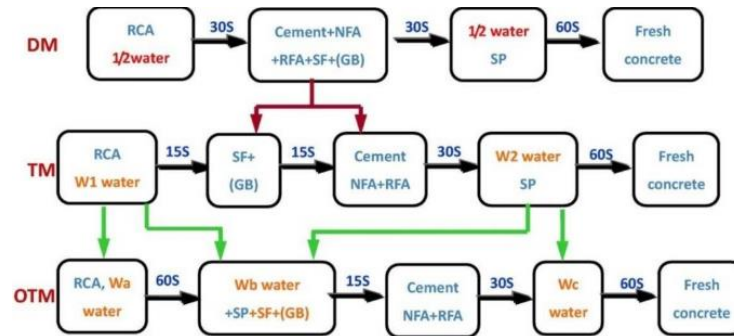


Figure 1. RAC  $Wb$  is the weight percentage of SCM's residual water in the gelling material overall;  $Wa$  is 60–80% of the product of RA's weight and water absorption; and  $Wc$  is the result of mixed water  $-Wb-Wa$

Table 1. Numerous elements' effects on RFA concrete's (RFAc) impermeability

Factor	Impact	Variation
RFA moisture level	Positive	Increase
Mineral additives	Positive	-
Enhanced triple mixing technique (OTM)	Positive	-
RFA proportion	Negative	Increase
Water-cement ratio	Negative	Increase

Research results show that our hybrid algorithm optimized neural network achieves precise compressive strength prognosis and provides sustainable mixtures with lower environmental effects. The manuscript establishes multiple new findings for both construction engineering science and environmental sustainability research. This manuscript proves the effectiveness of combining bio-inspired optimization methods for material assessment purposes in an atypical application domain. The research demonstrates that optimized SCMs have the potential to reduce greenhouse gas emissions substantially. The predictive features of this research will result in new modeling capabilities for planning and simulation tools to integrate directly into construction processes, thus enabling real-time, environmentally responsible material selection choices.

We will begin by providing an overview of the current state of cement manufacturing and its environmental impacts, highlighting the use of SCMs as a sustainable alternative. Following this, we will delve into the methodology section, outlining the hybrid optimization techniques and neural network models employed to enhance the predictive accuracy of concrete compressive strength. Subsequent sections will discuss the experimental setup, results, and a detailed analysis of the findings, focusing on the performance and generalizability of the model. Finally, we will conclude with a discussion on the implications of our research, future research directions, and the potential integration of our findings into a concrete mix design and quality control systems.

## 2. PREVIOUS WORK

Numerous studies on concrete technology have identified important factors and enhanced the prediction of concrete strength (CS) through the use of cutting-edge machine learning algorithms. For fly ash-based geopolymer concrete CS, decision tree algorithms, bagging, and AdaBoost regressors were used [102]. The bagging model made the best predictions, with an R-squared of 0.97. The most crucial CS characteristics were identified by a comprehensive sensitivity investigation, supporting the environmental sustainability of geopolymer concrete. Feng *et al.* [103] developed an intelligent CS prediction method based

on AdaBoost. Using AdaBoost, they outperformed artificial neural network (ANN) and support vector machine (SVM) on more than 1,030 case sets. In their article, they used sensitivity analysis and 10-fold cross-validation to calculate accuracy and precision. Research on recycling aggregate concrete (RAC) [104] using ANN symbolic learning and GEP. Sensitivity study revealed CS-affecting factors, and GEP performed better than ANN. Additionally, the study proposed that bagging and boosting might enhance prediction. SFRC beam shear resistance was predicted by many machine-learning algorithms [105]. The dependent variable was best predicted by XGBoost using tried-and-true machine learning techniques. Input parameters are anticipated in the study. Chen *et al.* [106] GBRT predicted concrete-FRP bond resistance. The best method and model, GBRT, predicted the issue. ANNs and genetic algorithms (Gas) or particle swarm optimization (PSO) predicted CES bond strength [107]. Test sensitivity analysis identified crucial variables. CS was evaluated at high temperatures using AdaBoost, Random Forests, and decision trees [108].

Highly cement sensitive, Gaussian process regression (GPR) with the Matern32 kernel function predicted high-performance concrete's CS better than ANNs [109]. In the sensitivity study, cement concentration and testing age were crucial. CS was predicted by Random Forest using field and lab data [110]. Field-trained models showed improved accuracy, indicating that several data sources reduce overprediction. Decision tree and gradient boosting tree models were used to examine the bending performance of FRP-reinforced concrete beams [111]. Beam depth, flexural reinforcement area, and assessment metrics supported the gradient-boosting tree model. ANNs, decision trees, Bagging, and gene expression programming predicted CS [112]. Bagging was most accurate at 0.95 R-squared.

The XGBoost model with manually selected features performed well in [113] when estimating CS based on concrete composition and cure period. According to the study, a decrease in dimensionality helps the support vector regression model. Machine-learning approaches were used to forecast setting time and strength development in Ordinary Portland cement binders [114]. The results were comparable to ASTM test methods. Finally, [115] tested ANN, boosting, and AdaBoost ensemble machine-learning approaches for geopolymers concrete CS prediction using high-calcium fly ash. Due to its accuracy, the boosting approach was acknowledged, and these findings suggest ensemble methods for enhancing concrete for sustainable development.

This study aims to improve concrete property forecasts. Improving predictive models requires understanding the intricate relationship between material components, ambient environments, and concrete physical properties. In the construction industry's quest for efficiency and sustainability, this study will enhance the prediction model's accuracy and adaptability through an analysis of environmental impacts and mechanical behaviors.

### 3. PROPOSED METHODOLOGY

This study uses extensive analysis, data management and manipulation methods, advanced artificial neural network architecture, and hybrid optimization algorithms. For optimal dataset use and high-quality findings, the dataset was cleaned and preprocessed using concrete properties. Data was normalized to reduce skewness in feature scales.

The neural network architecture served as the foundation for the built predictive model, which included convolutional and recurrent layers to extract the temporal relationships of the data in order to guarantee an accurate forecast of concrete strength. Because it provided a solid basis for further enhancements, this model arrangement was initially appropriate for testing performance.

The study advises creating FLA and dung beetle optimizers. This procedure improved model hyperparameter values more than normal. FLA effectively explores parameter space via global search optimization; DBOA finds the local optimum. A large solution space and reliable model prediction are guaranteed by comprehensive search approaches. Figure 2 shows the important methodology's application and linkages. Finally, the FLA+DBOA model's algorithm flow and predictive model integration are displayed in the following Figure 2.

In our methodology, we conducted a comprehensive dataset preprocessing to ensure the integrity and consistency of our model. The implementation of normalization standardized numerical values to match ranges while maintaining stability and convergence, through which the IQR method detected outliers to remove anomalous data that affected the analysis. The Min-Max scaler method was implemented for feature scaling in order to equalize the effects of each input feature upon model predictions.

Shapley additive explanations (SHAP) assessed the influence of different variables on concrete compressive strength predictions by assigning value weights to each contributing feature in the prediction. The predictive model gained both enhanced interpretability and transparency when using SHAP, which revealed vital features together with clearer explanations to increase the reliability of predictions.

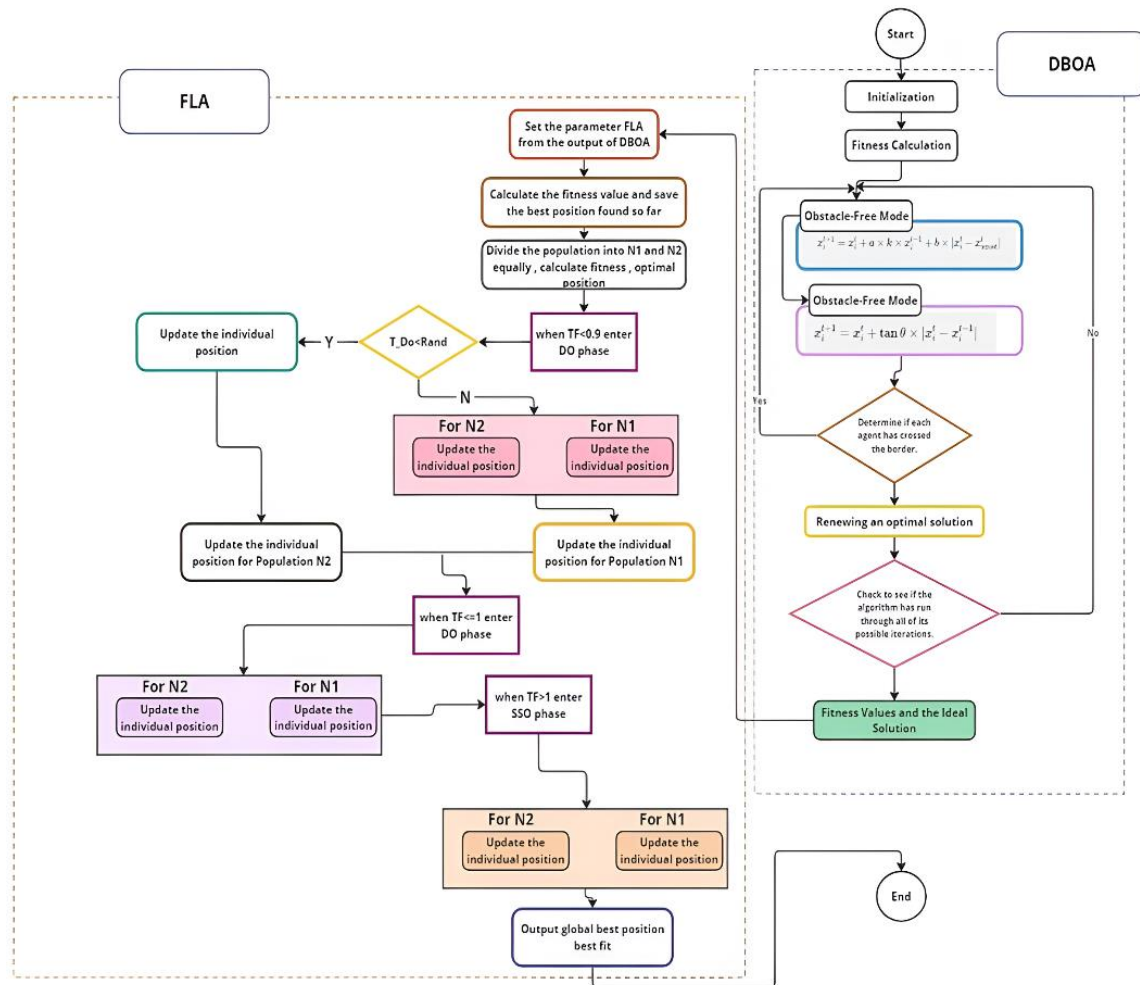


Figure 2. Proposed scheme

The model performed its training on hardware optimized for GPU computing to decrease processing time while attempting to scale the system. The design enables our system to process extended datasets effectively thus enabling practical applications that need immediate, precise outcomes. The implemented model relies on state-of-the-art computer tools and methods to guarantee computational productivity. A convolutional-recurrent neural network serves as our main computational element to process sequential and spatial concrete mix data efficiently. The model runs on a computing platform with powerful GPUs for its deployment. The specific configuration serves as an essential requirement to make deep learning models perform quickly during training and inference, thus enabling fast processing of big datasets and intricate operations. Using GPUs in the system enhances both processing speed and model scalability thus allowing the analysis of large datasets at high performance rates. The development process utilizes TensorFlow and Keras frameworks as optimized deep learning applications specifically designed for this purpose. The frameworks offer efficient neural network implementation, which includes automatic differentiation and GPU acceleration capabilities built right into their system. The provided support maximizes resource usage in order to enhance model speed and accuracy during computations. The computation process adopts standard software engineering principles that include logical modularization of code with optimized data arrays and parallel algorithm execution approaches. Model maintenance becomes simpler through these practices, while calculations run faster, and the system becomes ready for growth requirements.

The predictive accuracy of our model was validated through statistical tests that included t-tests and ANOVA for comparing different configuration results. The model performance was evaluated through an analysis that determined the effects of shifting GGBS or fly ash percentages. Our model required this evaluation to demonstrate its performance across various concrete mixed conditions as we aimed to generate robust findings applicable to different production scenarios.

The depiction in Figure 2 shows how the FLA and DBOA combine in a hybrid optimization structure without interruptions. The diagram shows how the iterative steps of the dual algorithm function through parameter establishment and population initial creation. The system computes fitness values to guide the search direction towards optimal solutions after this procedure.

The DBOA section allows the model to work without obstacles by readjusting individual positions through an equation designed for improved algorithm exploration. By detecting local minimum obstacles, the trajectory makes intended modifications that allow smooth navigation towards optimal solutions. The algorithm conducts a renewal procedure whenever it discovers an optimal solution, which allows it to perform more precise checks regarding boundary overstep from prior runs.

The FLA begins its hybrid system operations by establishing adjustable parameters that derive from DBOA outputs. A dynamic feedback mechanism created between the algorithms improves both adaptability and robustness during the optimization process. FLA separates its population across two groups, which conduct position updates based on fitness evaluations that are recalculated after every positional readjustment. The algorithm divides its execution into multiple phases, which activate when iteration counts reach their defined thresholds in order to achieve efficient exploration and exploitation of the search space.

Both algorithms update their strategies with each iteration using changes in search space conditions to reach their final identification of the global best position and fitness. This interactive algorithm mechanism both enhances individual algorithm effectiveness while utilizing their collective power to produce an optimized solution, which represents efficient management of exploration and exploitation resources needed for sophisticated optimization problems.

Our model evaluation includes examination of physics-informed machine learning (PIML) because we seek to elevate both interpretability and reliability of our predictive methods. PIML strengthens model outcomes by implementing domain knowledge into training because it enables users to understand how concrete mix design principles affect predictions, which leads to more accurate, trustworthy results. This method proves useful in material science because its analysis handles complex physical and chemical interactions that exhibit strong nonlinearity.

### 3.1. Dataset overview

The main dataset used for this study examines concrete mixtures as a whole system to understand how components work together during compression tests. The 1,030 samples have eight characteristics and one target variable. The type (10 classes) and age are also listed. With an average volume per mix of 281.17 kg, cement, the primary binder in concrete, is crucial to the structural behavior and longevity of the masonry industry.

Supplementary table cementitious materials average 73.90 kg blast furnace slag and 54.19kg fly ash. Read Intro. These improve durability and workability, but their proportions vary, providing a variety of experimental mixes. Water, which is needed for concrete workability and strength, weighs 181.57 kg per mix, whereas superplasticizers, which increase concrete fluidity without reducing strength, weigh 6.20 kilogram per mix. The bulk of the mix is composed of both coarse and fine aggregates, weighing 972.92 kg and 773.58 kg, respectively. These factors affect concrete texture, density, and strength. The average age of concrete samples was 45.66 days, representing a cure period, a key parameter for strength growth layers. Concrete undergoes chemical processes that release load-bearing properties. The average compressive strength, or load-carrying ability, of concrete is 35.82 MPa in this dataset. Other high-dimensional meta-features possess this scale, indicating aptitude for training predictive models that can handle many construction specifications and situations. In conclusion, the dataset helps estimate quench-flow composite compressive strength by measuring ingredients and weather conditions and monitoring difficult concrete mix interactions. This large data collection enables deeper examination of empirical relationships that affect concrete performance and customized mix designs for diverse construction applications.

In addition, we have included a comprehensive comparative Table 2 that details various optimization methods alongside the FLA and DBOA. Each optimization technique's accuracy, together with its computational timing and benefits and drawbacks, appears in this table, which includes particle swarm optimization (PSO) and genetic algorithm, and Bayesian optimization. An organized analysis enables better comprehension regarding why FLA and DBOA were selected for this research because of their particular advantages in resolving complex multi-dimensional optimization issues in concrete mixture design.

Our analysis of the dataset composition has been carried out to confirm the inclusion of diverse cement types across different geographic regions, which reduces biases related to materials and regions. This analysis confirms our model's ability to apply to various cement materials through different testing systems for sustainable global construction deployment.



Table 2. An overview of the concrete dataset's statistics

Feature	Count	Mean	Std Dev	Min	25%	50%	75%	Max
Cement	1030	281.17	104.51	102.00	192.38	272.90	350.00	540.00
Blast furnace slag	1030	73.90	86.28	0.00	0.00	22.00	142.95	359.40
Fly ash	1030	54.19	64.00	0.00	0.00	0.00	118.30	200.10
Water	1030	181.57	21.35	121.80	164.90	185.00	192.00	247.00
Superplasticizer	1030	6.20	5.97	0.00	0.00	6.40	10.20	32.20
Coarse aggregate	1030	972.92	77.75	801.00	932.00	968.00	1029.40	1145.00
Fine aggregate	1030	773.58	80.18	594.00	730.95	779.50	824.00	992.60
Age	1030	45.66	63.17	1.00	7.00	28.00	56.00	365.00
Strength (MPa)	1030	35.82	16.71	2.33	23.71	34.45	46.14	82.60

### 3.2. Preprocessing and exploratory data analysis

In the initial stage of empirical research, the concrete dataset and accurate processing were prioritized. The dataset was adjusted to scale all input features to similar ranges to generalize them and make neural network learning easier. Standardizing variables prevents the model from prioritizing features with greater numbers, balancing feature relevance.

Figure 3 presents a comprehensive analysis of the distribution of various concrete mix components through histograms, each detailing the frequency and range of one particular ingredient. The visualization begins with cement, displaying a right-skewed distribution that reflects a concentration of values at lower amounts with a gradual decline as the quantity increases. This pattern suggests that smaller amounts of cement are more commonly used in the mixtures within the dataset.

Moving to the blast furnace slag and fly ash histograms, both show a significant number of samples containing minimal to no amounts, highlighted by the sharp peaks at the lower end of the scale. These supplementary materials are applied on an optional basis or in minimal quantities across many concrete formulations found in the dataset.

The distribution shapes of water, along with superplasticizer and both coarse and fine aggregates, demonstrate typical usage patterns and value ranges within concrete mixtures. The water distribution indicates that most concrete mixes use amounts that fall near their median values. Superplasticizers are concentrated below the median amount, which shows many mixtures only use minimal amounts because this substance functions as an advanced additive rather than a regular mixture component.

Because of their essential role in the composition of concrete mixtures, coarse and fine aggregates appear to have a wide range of applications. Standards in curing periods have shaped the observed peaks within the age distribution since many concrete mixtures receive their prescribed curing durations.

Compressive strength data follows a normal distribution, giving evidence of typical concrete mix behavioral patterns in the tested samples. This visualization not only aids in understanding the typical properties of the materials used but also serves as a critical tool for identifying trends, anomalies, and the overall behavior of the components in concrete mix formulation.

Standardized exploratory data analysis (EDA) identified variable connections and distributions. The histograms in Figure 3 show that the "distribution of distribution" can be of any kind and that the data distribution differs for each data set. Because of low density at high cement concentration and denser locations at low cement levels, the cement feature displays a skewed right distribution. This skewness is important because cement determines the strength and durability of concrete.

At zero, the distribution of fly ash and blast furnace slag is noteworthy; thus, many mixtures do not use them. As shown by their widespread use in various fields, they can improve concrete properties.

Water is crucial to the concrete mix ratio, but most components are balanced. The right water levels affect curing, hydration, concrete strength, and movement. Superplasticizer is less popular than Frequent Limestone. Without water, mixed workability must be improved due to its increased frequency at lesser levels. Given that the bulk of concrete's volume is composed of coarse and fine aggregate, their distributions aid in explaining this. The variation in their quantities in the two samples suggests they can change mix density and strength.

Figure 4 correlation heatmap demonstrates a strong inverse relationship between water and superplasticizers, showing that superplasticizers reduce water use and strengthen mixes. In the line plot as shown in Figure 5, the positive correlation between Age and Strength emphasizes the necessity of curing, where strength grows with time. Concrete quality should be evaluated based on its age. These exploratory discoveries help optimize concrete mix designs for greater performance and sustainability in construction by understanding the intricate interaction of concrete components. This rigorous investigation illuminates concrete strength parameters, paving the road for building material science advancements.



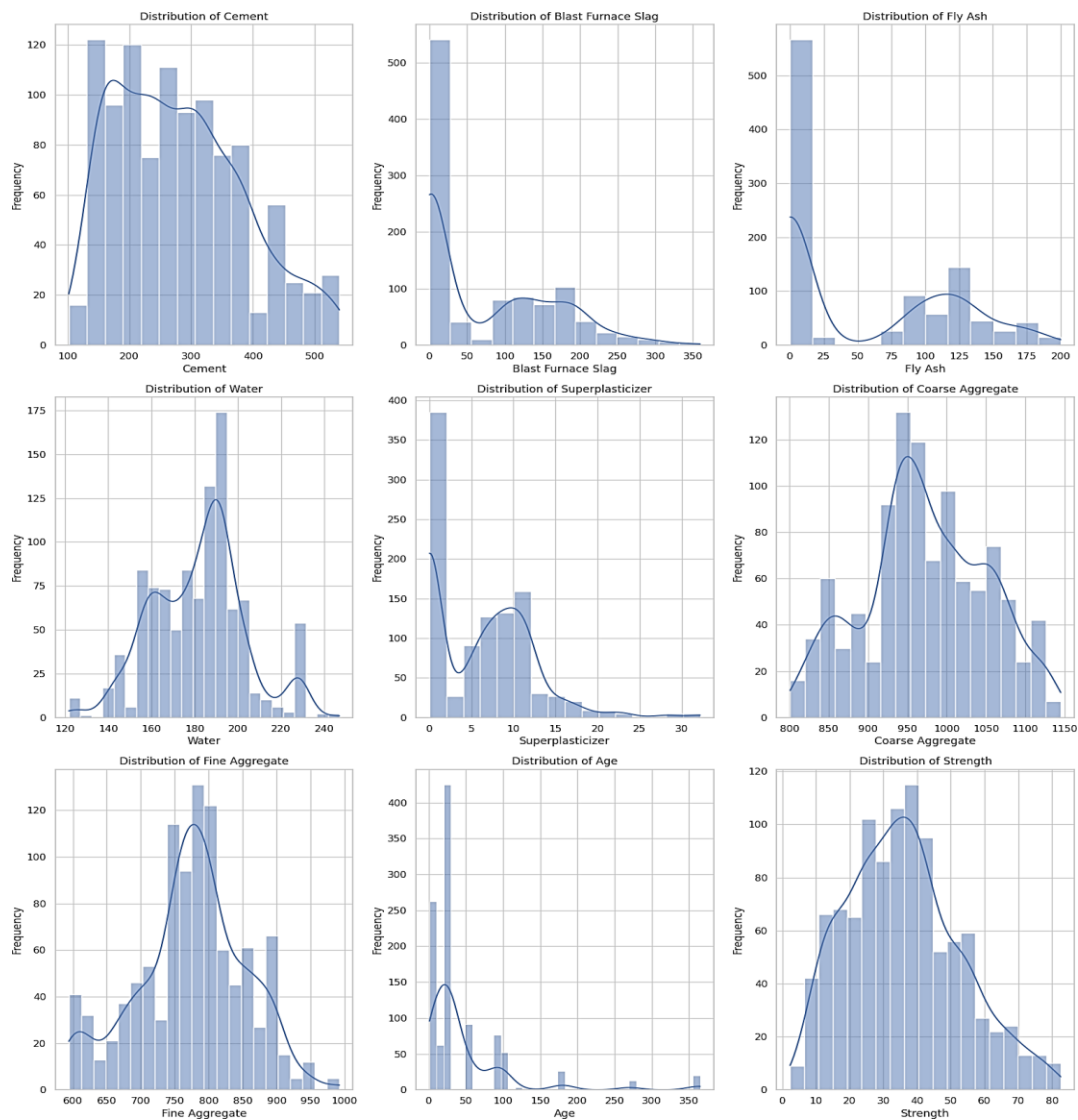


Figure 3. Histograms of concrete components

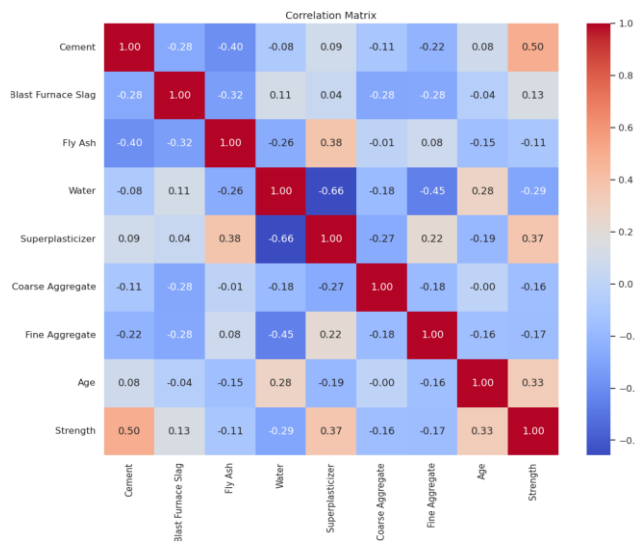


Figure 4. Concrete features correlation matrix

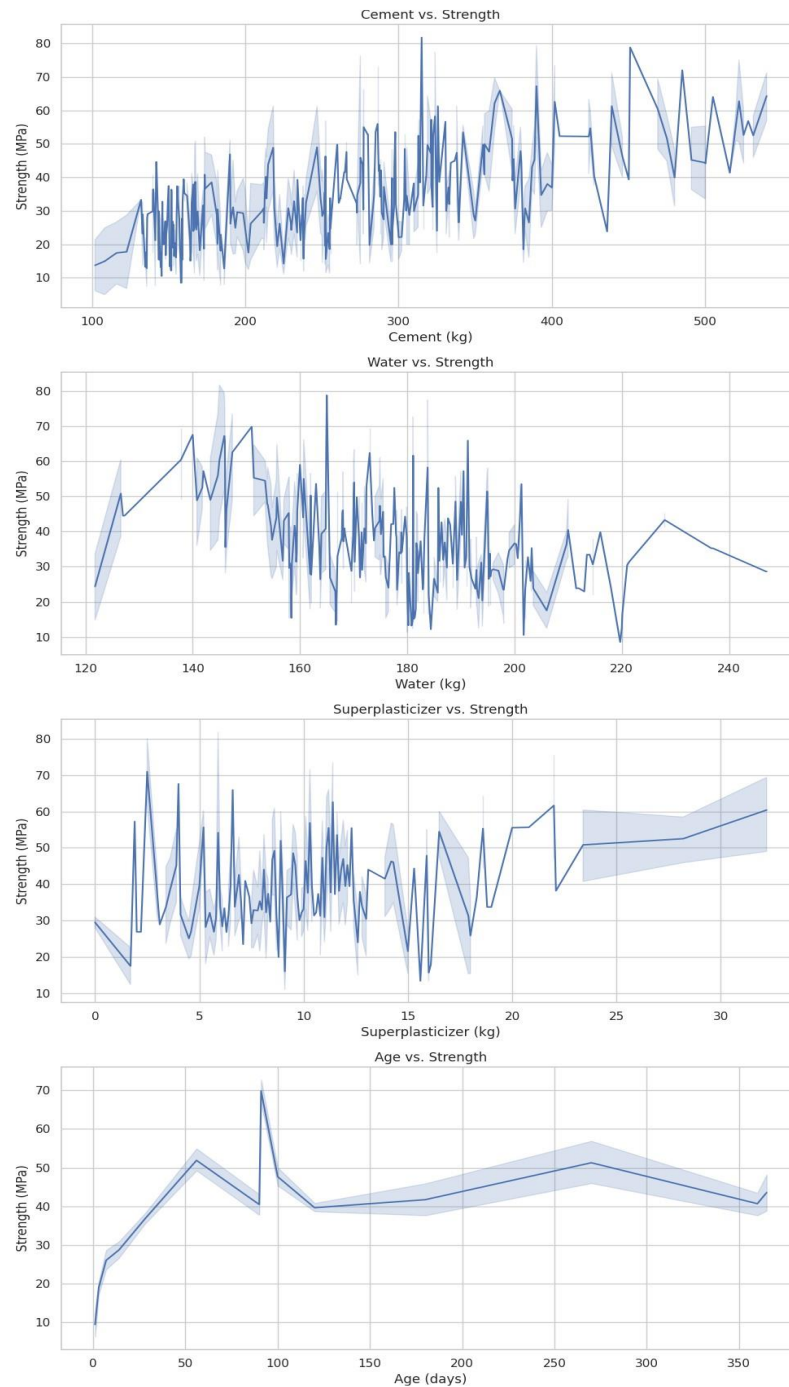


Figure 5. Impact of features on compressive strength

### 2.3. Hybrid convolutional-recurrent neural network (Conv1D-LSTM- GRU) architecture

Convolutional and recurrent neural networks manage sequential input and predict concrete strength using composition profiles and time sequence in Table 3. Layer one, a 1D convolutional layer, captures spatial relationships in the data. Two kernels and 64 filters comprised this layer. This reveals complicated patterns in sequential input data like concrete mix ingredient interactions. The model's bidirectional long short-term memory (LSTM) follows the convolutional layer. This layer has 50 LSTM units that can learn forward and backward dependencies. Processing data in both directions reduces the need to comprehend each data point's context, revealing patterns that one-directional analysis misses.

Adding a second bidirectional layer with GRU increases model complexity and capability. GRU contains 50 units and accepts two-way data like LSTM. GRUs are more effective and computationally

simpler, allowing faster training despite a modest performance difference. LSTM's general features are reduced to the most important for the final choice by this layer. The final layer is a thick network with one node for integrating characteristics and predicting concrete compressive strength. In this layer, the model employs a linear activation function for regression issues using actual output. The mean squared error loss function and Adam optimizer reduce training prediction errors, while backpropagation adjusts weights. In material science, this robust model is the best predictive analytical model as it captures data communication and general concrete strength features.

Table 3. Model values and parameters

Parameter	Value
Conv1D filters	64
Conv1D Kernel size	2
Bidirectional LSTM units	50
Bidirectional GRU units	50
Dense layer units	1
Optimizer	Adam
Loss function	Mean squared error
Total trainable parameters	91,893

## 2.4. FLA+DBOA hybrid

The hybrid optimization method uses the FLA and the DBOA to maximize the hyperparameters of neural network models. This hybrid approach completely explores and utilizes the search space using both approaches.

Step 1: Initialization

The first step is to generate a population of possible solutions. Every solution is represented by a vector of hyperparameters. The initial population is created at random for each parameter within predetermined limitations.

$$x_i = x_{i1}, x_{i2}, \dots, x_{in} \quad (1)$$

In this case, the  $i$ -th solution of the population is denoted by  $x_i$ , and the  $j$ -th parameter of the  $i$ -th solution by  $x_{ij}$ .

Step 2: Calculating fitness

Determine the goal function's fitness for every solution. The loss function of the neural network model is often the target function.

$$f(x_i) = \text{Loss}(x_i) \quad (2)$$

The neural network model's performance using the hyperparameters given by  $x_i$  is assessed by the fitness  $f(x_i)$ .

Step 3: Firefly algorithm (FLA) mechanism

The FLA component updates the population by simulating firefly activity. Brighter (better) solutions attract fireflies, and the path a firefly  $i$  follows to get close to another firefly  $j$  is determined by (3):

$$x_i^{(t+1)} = x_i^{(t)} + \beta e^{-\gamma r_{ij}^2} (x_j^{(t)} - x_i^{(t)}) + \alpha \epsilon_i \quad (3)$$

where  $\beta$  represents the attraction at  $r = 0$ . The symbol for the light absorption coefficient is  $\gamma$ . Fireflies  $i$  and  $j$  are separated by  $r_{ij}$ . The randomization parameter is denoted by  $\alpha$ . The vector  $\epsilon_i$  is random. In order to prevent local optima, this equation introduces randomization while guaranteeing that each firefly travels in the direction of brighter fireflies.

Step 4: Dung beetle optimizer algorithm (DBOA) mechanism

Through dung beetle simulation, the DBOA component refines the population. The ideal solution affects the direction and step size of solution  $x_i$ :

$$x_i^{(t+1)} = x_i^{(t)} + \theta (x_{best} - x_i^{(t)}) + \delta \epsilon_i \quad (4)$$

where  $\delta$  is an additional randomization parameter.  $\theta$  is a scaling factor. This approach ensures convergence towards an ideal solution by actively using the excellent areas that the firefly has found.

#### Step 5: Analyzing and choosing

Evaluate the solutions produced by FLA and DBOA for fitness. Update the optimal solution if the new one has a higher fitness value.

$$x_{\text{best}} = \operatorname{argmin} f(x_i) \quad (5)$$

#### Step 6: Iteration

Continue until a predefined number of iterations is reached or convergence conditions are satisfied. To arrive at the ideal neural network model hyperparameters, the solutions are improved over iterations.

### 4. EXPERIMENT RESULTS

Different models predict concrete compressive strength using the dataset, according to experiments as shown in Table 4. Dung beetle optimizer (DBO), firefly algorithm (FLA), and hybrid (DBO+FLA) optimized models are included. The baseline model, Conv1D-LSTM-GRU, has 49.006192 MSE, 5.690420 MAE, 7.000442 RMSE, and 0.809815 R2. These metrics quantify optimal model improvements.

The DBO model outperformed the baseline model with a test MSE of 44.015296, reducing prediction error. The DBO model had a smaller prediction error with a test MAE of 5.318566. Furthermore, a drop in the Test RMSE to 6.634402 indicated that the forecasts were more accurate. The test R2 increased to 0.829184, indicating a higher connection between the actual and projected compressive strengths.

As with FLA, performance improved. It had 44.748495 Test MSE, 5.326784 MAE, 6.689432 RMSE, and 0.826339 R2. The FLA model outperformed the baseline model in prediction accuracy and error reduction. DBO+FLA performed best in the experiment. According to Test MSE, the model has the lowest prediction error, 40.159906, and Test MAE was 5.148660, which is the lowest prediction error. Test RMSE reduced to 6.337184, improving forecast accuracy. With the highest test R2 of any model (0.844146), the predicted and real compressive strengths showed the best connection.

According to the experiment, the hybrid DBO+FLA model greatly enhances the ability to predict the compressive strength of concrete in Table 5. The DBO+FLA hybrid, in particular, is one of the optimum types, showing how modern optimization methods refine neural network hyperparameters, improving material science predictions. Comparing our results to related works, because of the size of our dataset, error measurements like root mean squared error (RMSE) and mean squared error (MSE) may rise. Bigger datasets are more complicated and varied, which makes prediction more difficult and raises absolute error levels. However, our hybrid optimization strategy is robust and effective because our models improve consistently.

Table 4. Results of the forecasting test for concrete compressive strength

Model	Test MSE	Test MAE	Test RMSE	Test R2
Conv1D-LSTM-GRU	49.006192	5.690420	7.000442	0.809815
DBO	44.015296	5.318566	6.634402	0.829184
FLA	44.748495	5.326784	6.689432	0.826339
<b>DBO+FLA</b>	<b>40.159906</b>	<b>5.148660</b>	<b>6.337184</b>	<b>0.844146</b>

Table 5. Comparing the outcomes of the experiment with related works

Ref.	RMSE	R <sup>2</sup>	MSE	MAE	EV	MAPE
AdaBoost [109]	-	0.938	-	-	-	12.523
Boosting [103]	1.94	-	3.75	1.51	-	-
Bagging [113]	4.97	-	24.76	3.69	-	-
model_1 <b>Our Work</b>	7.00	0.81	49.01	5.69	-	-
DBO <b>Our Work</b>	6.63	0.83	44.02	5.32	-	-
FLA <b>Our Work</b>	6.69	0.83	44.75	5.33	-	-
DBO+FLA <b>Our Work</b>	6.34	0.84	40.16	5.15	-	-

The superiority of the developed models is underscored by the integration of the FLA and DBOA with a convolutional-recurrent neural network, offering significant enhancements over traditional modeling approaches. This hybrid optimization approach combines the accuracy of DBOA's local search with FLA's global search power, allowing the model to more successfully traverse intricate optimization landscapes and steer clear of local minima. Enhanced accuracy happens when predicting concrete compressive strength because of this method, which is vital for reliable construction material assessment.

The convolutional-recurrent architecture successfully detects spatial and temporal dependencies that naturally exist in concrete mix databases. Organizations depend on this functionality to understand complex interactions that impact the material properties of concrete components. The model demonstrates robustness through successful adoption across different datasets, which enables performance maintenance across various operational conditions. The developed models benefit from efficient operation since GPU acceleration supports the preservation of high computational efficiency, together with accurate prediction speed. The system delivers outstanding benefits to industries that require rapid resource management and quick execution times.

The adoption of SHAP among feature analysis methods brings both enhanced model interpretability as well as transparency. The model gains wider practical use because users and decision-makers develop trust through feature explanation while gaining comprehension of which input elements lead to specific output predictions. The extensive understanding of model prediction reasons stands equally important to prediction accuracy, thus making model transparency an essential matter for specific sectors. When combined, these architectural elements demonstrate a major improvement in utilizing machine learning algorithms to forecast concrete strength, which results in outstanding operational effectiveness for practical and industrial use.

## 5. CONCLUSION

The project investigates methods of reducing CO<sub>2</sub> emissions from the construction sector by enhancing concrete properties through the use of supplementary cementitious materials (SCMs), such as ground granulated blast furnace slag (GGBS) and fly ash (FA). The prediction of concrete compressive strength has increased thanks to thorough data analysis and potent machine learning techniques. The hybrid optimization method fine-tuned Convolutional-Recurrent Neural Network hyperparameters using the FLA and DBOA. It optimized the model better than earlier methods. Of all the models tested, the hybrid model scored the lowest MSE, RMSE, and R<sup>2</sup>. Our results show that FLA and DBOA work well for accuracy in material science forecasting. The hybrid method fully uses the hyperparameter search space for more accurate predictions. SCMs in concrete mixtures benefit the building industry's low-carbon circular economy. Finally, this research offers a new way to optimize concrete mix designs, adding to sustainable construction expertise. The results demonstrate that advanced optimization and SCMs may enhance material performance and environmental sustainability. To enhance them, future studies may apply these strategies to more concrete manufacturing processes and incorporate further optimization approaches.

## FUNDING INFORMATION

Authors state no funding involved.

## AUTHOR CONTRIBUTIONS STATEMENT

This journal uses the Contributor Roles Taxonomy (CRediT) to recognize individual author contributions, reduce authorship disputes, and facilitate collaboration.

Name of Author	C	M	So	Va	Fo	I	R	D	O	E	Vi	Su	P	Fu
Esra'a Alhenawi	✓	✓	✓	✓	✓	✓	✓	✓	✓	✓	✓	✓	✓	
Ayat Mahmoud Al-Hinawi	✓	✓		✓		✓	✓	✓	✓	✓	✓	✓	✓	
Zaher Salah	✓	✓	✓	✓	✓		✓	✓	✓	✓	✓	✓	✓	
Omar Alidmat	✓	✓	✓	✓	✓		✓	✓	✓	✓	✓	✓	✓	
Esraa Abu Elsoud	✓	✓	✓	✓	✓		✓	✓		✓	✓	✓	✓	
Raed Alazaidah	✓	✓	✓	✓	✓		✓	✓		✓	✓	✓	✓	
Bashar Rizik AlSayyed	✓	✓	✓	✓	✓		✓	✓	✓		✓	✓	✓	

C : **C**onceptualization

M : **M**ethodology

So : **S**oftware

Va : **V**alidation

Fo : **F**ormal analysis

I : **I**nvestigation

R : **R**esources

D : **D**ata Curation

O : Writing - **O**riginal Draft

E : Writing - Review & **E**ditng

Vi : **V**isualization

Su : **S**upervision

P : **P**roject administration

Fu : **F**unding acquisition

## CONFLICT OF INTEREST STATEMENT

Authors state no conflict of interest.

## DATA AVAILABILITY

The data that support the findings of this study are available from the corresponding author, ZS, upon reasonable request.

## REFERENCES

- [1] R. Prakash, R. Thenmozhi, and S. N. Raman, "Mechanical characterisation and flexural performance of eco-friendly concrete produced with fly ash as cement replacement and coconut shell coarse aggregate," *International Journal of Environment and Sustainable Development*, vol. 18, no. 2, pp. 131–148, 2019, doi: 10.1504/IJESD.2019.099491.
- [2] R. Prakash, R. Thenmozhi, S. N. Raman, and C. Subramanian, "Characterization of eco-friendly steel fiber-reinforced concrete containing waste coconut shell as coarse aggregates and fly ash as partial cement replacement," *Structural Concrete*, vol. 21, no. 1, pp. 437–447, 2020, doi: 10.1002/suco.201800355.
- [3] J. Ahmad *et al.*, "A comprehensive review on the ground granulated blast furnace slag (GGBS) in concrete production," *Sustainability (Switzerland)*, vol. 14, no. 14, 2022, doi: 10.3390/su14148783.
- [4] J. M. M. Provis, A. M. Sabbie, and H. Arpad, "Towards sustainable concrete," *Nature Materials*, vol. 16, pp. 698–699, 2017.
- [5] J. G. J. Olivier and P. J.A.H.W., "Trends in global CO<sub>2</sub> and total greenhouse gas emissions," *PBL Netherlands Environmental Assessment Agency*, no. December, pp. 1–85, 2020.
- [6] O. Smirnova, "Compatibility of shungisite microfillers with polycarboxylate admixtures in cement compositions," *ARPJ Journal of Engineering and Applied Sciences*, vol. 14, no. 3, pp. 600–610, 2019.
- [7] T. Bakharev, "Geopolymeric materials prepared using class F fly ash and elevated temperature curing," *Cement and Concrete Research*, vol. 35, no. 6, pp. 1224–1232, 2005, doi: 10.1016/j.cemconres.2004.06.031.
- [8] M. J. Mwititi, T. J. Karanja, and W. J. Muthengia, "Thermal resistivity of chemically activated calcined clays-based cements," *RILEM Bookseries*, vol. 16, pp. 327–333, 2018, doi: 10.1007/978-94-024-1207-9\_53.
- [9] O. M. Smirnova, I. M. P. de Navascués, V. R. Mikhailevskii, O. I. Kolosov, and N. S. Skolota, "Sound-absorbing composites with rubber crumb from used tires," *Applied Sciences (Switzerland)*, vol. 11, no. 16, 2021, doi: 10.3390/app11167347.
- [10] D. De Domenico, F. Faleschini, C. Pellegrino, and G. Ricciardi, "Structural behavior of RC beams containing EAF slag as recycled aggregate: Numerical versus experimental results," *Construction and Building Materials*, vol. 171, pp. 321–337, 2018, doi: 10.1016/j.conbuildmat.2018.03.128.
- [11] J. J. Brooks and M. A. Megat Johari, "Effect of metakaolin on creep and shrinkage of concrete," *Cement and Concrete Composites*, vol. 23, no. 6, pp. 495–502, 2001, doi: 10.1016/S0958-9465(00)00095-0.
- [12] N. Bheel *et al.*, "Fresh and hardened properties of concrete incorporating binary blend of metakaolin and ground granulated blast furnace slag as supplementary cementitious material," *Advances in Civil Engineering*, vol. 2020, 2020, doi: 10.1155/2020/8851030.
- [13] S. I. Khassaf, A. T. Jasim, and F. K. Mahdi, "Investigation the properties of concrete containing rice husk ash to reduction the seepage in canals," *International Journal of Scientific & Technology Research*, vol. 3, no. 4, pp. 348–354, 2014.
- [14] D. D. Burduhos Nergis, P. Vizureanu, and O. Corbu, "Synthesis and characteristics of local fly ash based geopolymers mixed with natural aggregates," *Revista de Chimie*, vol. 70, no. 4, pp. 1262–1267, 2019, doi: 10.37358/rc.19.4.7106.
- [15] P. Ganesh and A. R. Murthy, "Tensile behaviour and durability aspects of sustainable ultra-high performance concrete incorporated with GGBS as cementitious material," *Construction and Building Materials*, vol. 197, pp. 667–680, 2019, doi: 10.1016/j.conbuildmat.2018.11.240.
- [16] E. Crossin, "The greenhouse gas implications of using ground granulated blast furnace slag as a cement substitute," *Journal of Cleaner Production*, vol. 95, pp. 101–108, 2015, doi: 10.1016/j.jclepro.2015.02.082.
- [17] İ. Şanal, "Fresh-state performance design of green concrete mixes with reduced carbon dioxide emissions," *Greenhouse Gases: Science and Technology*, vol. 8, no. 6, pp. 1134–1145, 2018, doi: 10.1002/ghg.1826.
- [18] A. Gholampour and T. Ozbakkaloglu, "Performance of sustainable concretes containing very high volume class-F fly ash and ground granulated blast furnace slag," *Journal of Cleaner Production*, vol. 162, pp. 1407–1417, 2017, doi: 10.1016/j.jclepro.2017.06.087.
- [19] H. Zhao, W. Sun, X. Wu, and B. Gao, "The properties of the self-compacting concrete with fly ash and ground granulated blast furnace slag mineral admixtures," *Journal of Cleaner Production*, vol. 95, pp. 66–74, 2015, doi: 10.1016/j.jclepro.2015.02.050.
- [20] M. Abbass, D. Singh, and G. Singh, "Properties of hybrid geopolymer concrete prepared using rice husk ash, fly ash and GGBS with coconut fiber," *Materials Today: Proceedings*, vol. 45, pp. 4964–4970, 2021, doi: 10.1016/j.matpr.2021.01.390.
- [21] S. Prakash, S. Kumar, R. Biswas, and B. Rai, "Influence of silica fume and ground granulated blast furnace slag on the engineering properties of ultra-high-performance concrete," *Innovative Infrastructure Solutions*, vol. 7, no. 1, 2022, doi: 10.1007/s41062-021-00714-7.
- [22] V. B. R. Suda and P. S. Rao, "Experimental investigation on optimum usage of Micro silica and GGBS for the strength characteristics of concrete," *Materials Today: Proceedings*, vol. 27, pp. 805–811, 2020, doi: 10.1016/j.matpr.2019.12.354.
- [23] S. VEDIYAPPAN, P. K. Chinnaraj, B. B. Hanumantraya, and S. K. Subramanian, "An experimental investigation on geopolymer concrete utilising micronized biomass silica and GGBS," *KSCCE Journal of Civil Engineering*, vol. 25, no. 6, pp. 2134–2142, 2021, doi: 10.1007/s12205-021-1477-8.
- [24] H. K. Hamzah, G. F. Huseien, M. A. Asaad, D. P. Georgescu, S. K. Ghoshal, and F. Alrshoudi, "Effect of waste glass bottles-derived nanopowder as slag replacement on mortars with alkali activation: Durability characteristics," *Case Studies in Construction Materials*, vol. 15, 2021, doi: 10.1016/j.cscm.2021.e00775.
- [25] J. Ahmad *et al.*, "Effects of steel fibers (SF) and ground granulated blast furnace slag (GGBS) on recycled aggregate concrete," *Materials*, vol. 14, no. 24, 2021, doi: 10.3390/ma14247497.
- [26] R. Yu, P. Spiesz, and H. J. H. Brouwers, "Development of an eco-friendly ultra-high performance concrete (UHPC) with efficient cement and mineral admixtures uses," *Cement and Concrete Composites*, vol. 55, pp. 383–394, 2015, doi: 10.1016/j.cemconcomp.2014.09.024.
- [27] S. C. Pal, A. Mukherjee, and S. R. Pathak, "Investigation of hydraulic activity of ground granulated blast furnace slag in concrete," *Cement and Concrete Research*, vol. 33, no. 9, pp. 1481–1486, 2003, doi: 10.1016/S0008-8846(03)00062-0.
- [28] K. Y. Yea and E. K. Kim, "An experimental study on corrosion resistance of concrete with ground granulate blast-furnace slag," *Cement and Concrete Research*, vol. 35, no. 7, pp. 1391–1399, 2005, doi: 10.1016/j.cemconres.2004.11.010.
- [29] S. Teng, T. Y. D. Lim, and B. Sabet Divsholi, "Durability and mechanical properties of high strength concrete incorporating ultra

- fine ground granulated blast-furnace slag,” *Construction and Building Materials*, vol. 40, pp. 875–881, 2013, doi: 10.1016/j.conbuildmat.2012.11.052.
- [30] B. P. Lenka, R. K. Majhi, S. Singh, and A. N. Nayak, “Eco-friendly and cost-effective concrete utilizing high-volume blast furnace slag and demolition waste with lime,” *European Journal of Environmental and Civil Engineering*, vol. 26, no. 11, pp. 5351–5373, 2022, doi: 10.1080/19648189.2021.1896581.
- [31] H. Constantinescu, O. Gherman, C. Negrutiu, and S. P. Ioan, “Mechanical properties of hardened high strength concrete,” *Procedia Technology*, vol. 22, pp. 219–226, 2016, doi: 10.1016/j.protcy.2016.01.047.
- [32] S. Jercan, “Concrete roads,” *Corvin Publishing House*. Romania, 2002.
- [33] L. Nicolescu, “Hydrotechnical concretes for land improvement works,” Publishing house CERES, Romania, 1997.
- [34] A. M. Neville, “Properties of concrete,” Bucharest Technical Publishing House, Romania, 1979.
- [35] I. Teoreanu, “Technology of binders and concretes,” Didactic and Pedagogical Publishing House, Romania, 1967.
- [36] L. Iureş, “Research report: Concretes with reduced shrinkage made with special additives,” *Journal of Science Policy and Scientometrics - Special Issue 2005*, pp. 1218–1582, 2005.
- [37] R. A. Medeiros, M. G. Lima, R. Yazigi, and M. H. F. Medeiros, “Carbonation depth in 57 years old concrete structures,” *Steel and Composite Structures*, vol. 19, no. 4, pp. 953–966, 2015, doi: 10.12989/scs.2015.19.4.953.
- [38] G. Kim, J. Y. Kim, K. E. Kurtis, L. J. Jacobs, Y. Le Pape, and M. Guimaraes, “Quantitative evaluation of carbonation in concrete using nonlinear ultrasound,” *Materials and Structures/Materiaux et Constructions*, vol. 49, no. 1–2, pp. 399–409, 2016, doi: 10.1617/s11527-014-0506-1.
- [39] Vagelis G. Papadakis, Costas G. Vayenas, and Michael N. Fardis, “Fundamental modeling and experimental investigation of concrete carbonation,” *ACI Materials Journal*, vol. 88, no. 4, 1991.
- [40] V. G. Papadakis, C. G. Vayenas, and M. N. Fardis, “Experimental investigation and mathematical modeling of the concrete carbonation problem,” *Chemical Engineering Science*, vol. 46, no. 5–6, pp. 1333–1338, 1991, doi: 10.1016/0009-2509(91)85060-B.
- [41] F. Pacheco-Torgal, Y. Ding, and S. Jalali, “Properties and durability of concrete containing polymeric wastes (tyre rubber and polyethylene terephthalate bottles): An overview,” *Construction and Building Materials*, vol. 30, pp. 714–724, 2012, doi: 10.1016/j.conbuildmat.2011.11.047.
- [42] J. D. Rios, A. Vahi, C. Leiva, A. M. Martínez-De la Concha, and H. Cifuentes, “Analysis of the utilization of air-cooled blast furnace slag as industrial waste aggregates in self-compacting concrete,” *Sustainability (Switzerland)*, vol. 11, no. 6, 2019, doi: 10.3390/su11061702.
- [43] O. Corbu, A. Puskás, A. V. Sandu, A. M. Ioani, H. Kamarudin, and I. G. Sandu, “New concrete with recycled aggregates from leftover concrete,” *Applied Mechanics and Materials*, vol. 754–755, pp. 389–394, 2015, doi: 10.4028/www.scientific.net/amm.754-755.389.
- [44] R. K. Majhi, A. N. Nayak, and B. B. Mukharjee, “Characterization of lime activated recycled aggregate concrete with high-volume ground granulated blast furnace slag,” *Construction and Building Materials*, vol. 259, 2020, doi: 10.1016/j.conbuildmat.2020.119882.
- [45] A. Forton, S. Mangiafico, C. Sauzéat, H. Di Benedetto, and P. Marc, “Behaviour of binder blends: experimental results and modelling from LVE properties of pure binder, RAP binder and rejuvenator,” *Road Materials and Pavement Design*, vol. 22, no. S1, pp. S197–S213, 2021, doi: 10.1080/14680629.2021.1905699.
- [46] R. D. Cadar, R. M. Boitor, and M. L. Dragomir, “An analysis of reclaimed asphalt pavement from a single source—case study: A secondary road in romania,” *Sustainability (Switzerland)*, vol. 14, no. 12, 2022, doi: 10.3390/su14127057.
- [47] A. Forton, S. Mangiafico, C. Sauzéat, H. Di Benedetto, and P. Marc, “Properties of blends of fresh and RAP binders with rejuvenator: Experimental and estimated results,” *Construction and Building Materials*, vol. 236, 2020, doi: 10.1016/j.conbuildmat.2019.117555.
- [48] Y. Soni and N. Gupta, “Experimental investigation on workability of concrete with partial replacement of cement by ground granulated blast furnace and sand by quarry dust,” *IJIRST-International Journal for Innovative Research in Science & Technology*, vol. 3, no. 04, pp. 312–316, 2016.
- [49] L. M. Molnar, D. L. Manea, C. Aciu, and E. Jumate, “Innovative plastering mortars based on recycled waste glass,” *Procedia Technology*, vol. 19, pp. 299–306, 2015, doi: 10.1016/j.protcy.2015.02.043.
- [50] T. Ozbakkaloglu, L. Gu, and A. Fallah Pour, “Normal- and high-strength concretes incorporating air-cooled blast furnace slag coarse aggregates: Effect of slag size and content on the behavior,” *Construction and Building Materials*, vol. 126, pp. 138–146, 2016, doi: 10.1016/j.conbuildmat.2016.09.015.
- [51] Q. Cao, U. Nawaz, X. Jiang, L. Zhanga, and W. S. Ansari, “Effect of air-cooled blast furnace slag aggregate on mechanical properties of ultra-high-performance concrete,” *Case Studies in Construction Materials*, vol. 16, 2022, doi: 10.1016/j.cscm.2022.e01027.
- [52] D. Popescu and A. Burlacu, “Considerations on the benefits of using recyclable materials for road construction,” *Romanian Journal of Transport Infrastructure*, vol. 6, no. 1, pp. 43–53, 2017, doi: 10.1515/rjti-2017-0053.
- [53] Concrete Urinary of JSCE, “Guidelines for construction using blast-furnace slag aggregate concrete,” *JSCE*, 1993. <https://www.jsce.or.jp/committee/concrete/e/web/pdf/22-2.pdf> (accessed Feb. 16, 2023).
- [54] ASA 36pp Guide—(Iron & Steel) Slag Association, “A guide to the use of slag in roads.” <https://www.yumpu.com/en/document/view/20477792/asa-36pp-guide-iron-steel-slag-association> (accessed Feb. 16, 2023).
- [55] A. Burlacu and C. Racanel, “Reducing cost of infrastructure works using new technologies,” in *Proceedings of the 3rd International Conference on Road and Rail Infrastructure – CETRA 2014: Road and Rail Infrastructure III*, 2014, pp. 189–194.
- [56] C. Dimulescu and A. Burlacu, “Industrial waste materials as alternative fillers in asphalt mixtures,” *Sustainability (Switzerland)*, vol. 13, no. 14, 2021, doi: 10.3390/su13148068.
- [57] A. Kumar and K. Deep, “Experimental investigation of concrete with cementitious waste material such as GGBS & fly ash over conventional concrete,” *Materials Today: Proceedings*, vol. 74, pp. 953–961, 2023, doi: 10.1016/j.matpr.2022.11.297.
- [58] P. Magudeaswaran, Vivek Kumar C, K. Vamsi Krishna, A. Nagasaibaba, and R. Ravinder, “Investigational studies on the impact of supplementary cementitious materials (SCM) for identifying the strength and durability characteristics in self curing concrete,” *Materials Today: Proceedings*, 2023, doi: 10.1016/j.matpr.2023.03.161.
- [59] M. H. Zhang and Canmet, “Microstructure, crack propagation, and mechanical properties of cement pastes containing high volumes of fly ashes,” *Cement and Concrete Research*, vol. 25, no. 6, pp. 1165–1178, 1995, doi: 10.1016/0008-8846(95)00109-P.
- [60] I. De La Varga, R. P. Spragg, C. Di Bella, J. Castro, D. P. Bentz, and J. Weiss, “Fluid transport in high volume fly ash mixtures with and without internal curing,” *Cement and Concrete Composites*, vol. 45, pp. 102–110, 2014, doi: 10.1016/j.cemconcomp.2013.09.017.
- [61] Z. T. Yao *et al.*, “A comprehensive review on the applications of coal fly ash,” *Earth-Science Reviews*, vol. 141, pp. 105–121, 2015, doi: 10.1016/j.earscirev.2014.11.016.






- [62] K. Celik, C. Meral, M. Mancio, P. K. Mehta, and P. J. M. Monteiro, "A comparative study of self-consolidating concretes incorporating high-volume natural pozzolan or high-volume fly ash," *Construction and Building Materials*, vol. 67, pp. 14–19, 2014, doi: 10.1016/j.conbuildmat.2013.11.065.
- [63] V. M. Malhotra and P. K. Mehta, "High-performance high-volume fly ash concrete," *Concrete International*, p. 101, 2002.
- [64] Malhotra, V.M. and P. K. Mehta(2005), "High-performance, high-volume fly ash concrete for sustainable development," *International Workshop on Sustainable Development and Concrete Technology*, 2004.
- [65] M. Şahmaran, I. Ö. Yaman, and M. Tokyay, "Transport and mechanical properties of self consolidating concrete with high volume fly ash," *Cement and Concrete Composites*, vol. 31, no. 2, pp. 99–106, 2009, doi: 10.1016/j.cemconcomp.2008.12.003.
- [66] P. Dinakar, K. G. Babu, and M. Santhanam, "Durability properties of high volume fly ash self compacting concretes," *Cement and Concrete Composites*, vol. 30, no. 10, pp. 880–886, 2008, doi: 10.1016/j.cemconcomp.2008.06.011.
- [67] N. Bouzoubaâ, A. Bilodeau, B. Tamtsia, and S. Foo, "Carbonation of fly ash concrete: Laboratory and field data," *Canadian Journal of Civil Engineering*, vol. 37, no. 12, pp. 1535–1549, 2010, doi: 10.1139/L10-081.
- [68] A. Mardani-Aghabaglou and K. Ramyar, "Mechanical properties of high-volume fly ash roller compacted concrete designed by maximum density method," *Construction and Building Materials*, vol. 38, pp. 356–364, 2013, doi: 10.1016/j.conbuildmat.2012.07.109.
- [69] H. J. Chen, N. H. Shih, C. H. Wu, and S. K. Lin, "Effects of the loss on ignition of fly ash on the properties of high-volume fly ash concrete," *Sustainability (Switzerland)*, vol. 11, no. 9, 2019, doi: 10.3390/sul1092704.
- [70] W. Müllauer, R. E. Beddoe, and D. Heinz, "Leaching behaviour of major and trace elements from concrete: Effect of fly ash and GGBS," *Cement and Concrete Composites*, vol. 58, pp. 129–139, 2015, doi: 10.1016/j.cemconcomp.2015.02.002.
- [71] L. Wang, Y. Huang, F. Zhao, T. Huo, E. Chen, and S. Tang, "Comparison between the influence of finely ground phosphorous slag and fly ash on frost resistance, pore structures and fractal features of hydraulic concrete," *Fractal and Fractional*, vol. 6, no. 10, 2022, doi: 10.3390/fractalfract6100598.
- [72] L. Wang *et al.*, "The influence of fly ash dosages on the permeability, pore structure and fractal features of face slab concrete," *Fractal and Fractional*, vol. 6, no. 9, 2022, doi: 10.3390/fractalfract6090476.
- [73] T. Boubekur, B. Boulekbache, K. Aoudjane, K. Eziane, and E. H. Kadri, "Prediction of the durability performance of ternary cement containing limestone powder and ground granulated blast furnace slag," *Construction and Building Materials*, vol. 209, pp. 215–221, 2019, doi: 10.1016/j.conbuildmat.2019.03.120.
- [74] Y. Jeong, H. Park, Y. Jun, J. H. Jeong, and J. E. Oh, "Microstructural verification of the strength performance of ternary blended cement systems with high volumes of fly ash and GGBFS," *Construction and Building Materials*, vol. 95, pp. 96–107, 2015, doi: 10.1016/j.conbuildmat.2015.07.158.
- [75] J. S. Lim, C. B. Cheah, and M. B. Ramli, "The setting behavior, mechanical properties and drying shrinkage of ternary blended concrete containing granite quarry dust and processed steel slag aggregate," *Construction and Building Materials*, vol. 215, pp. 447–461, 2019, doi: 10.1016/j.conbuildmat.2019.04.162.
- [76] "V.B.R. Suda and P. Srinivasa Rao. Experimental investigation on optimum usage of micro silica and ggbs for the strength characteristics of concrete. Materials Proceedings, 27:805–811, 2020."
- [77] A. A. Shubbar, H. Jafer, A. Dulaimi, K. Hashim, W. Atherton, and M. Sadique, "The development of a low carbon binder produced from the ternary blending of cement, ground granulated blast furnace slag and high calcium fly ash: An experimental and statistical approach," *Construction and Building Materials*, vol. 187, pp. 1051–1060, 2018, doi: 10.1016/j.conbuildmat.2018.08.021.
- [78] C. B. Cheah, J. J. Liew, K. Khaw Le Ping, R. Siddique, and W. Tangchirapat, "Properties of ternary blended cement containing ground granulated blast furnace slag and ground coal bottom ash," *Construction and Building Materials*, vol. 315, 2022, doi: 10.1016/j.conbuildmat.2021.125249.
- [79] R. Shamass, O. Rispoli, V. Limbachiya, and R. Kovacs, "Mechanical and GWP assessment of concrete using blast furnace slag, silica fume and recycled aggregate," *Case Studies in Construction Materials*, vol. 18, 2023, doi: 10.1016/j.cscm.2023.e02164.
- [80] K. Weise, N. Ukrainczyk, A. Duncan, and E. Koenders, "Enhanced metakaolin reactivity in blended cement with additional calcium hydroxide," *Materials*, vol. 15, no. 1, 2022, doi: 10.3390/ma15010367.
- [81] M. Izadifar *et al.*, "Comprehensive examination of dehydroxylation of kaolinite, disordered kaolinite, and dickite: Experimental studies and density functional theory," *Clays and Clay Minerals*, vol. 68, no. 4, pp. 319–333, 2020, doi: 10.1007/s42860-020-00082-w.
- [82] A. Barbucci, M. Delucchi, and G. Cerisola, "Organic coatings for concrete protection: Liquid water and water vapour permeabilities," *Progress in Organic Coatings*, vol. 30, no. 4, pp. 293–297, 1997, doi: 10.1016/S0300-9440(97)00007-6.
- [83] Y. Wang, G. Chen, B. Wan, H. Lin, and J. Zhang, "Behavior of innovative circular ice filled steel tubular stub columns under axial compression," *Construction and Building Materials*, vol. 171, pp. 680–689, 2018, doi: 10.1016/j.conbuildmat.2018.03.208.
- [84] A. Brenna, F. Bolzoni, S. Beretta, and M. Ormellese, "Long-term chloride-induced corrosion monitoring of reinforced concrete coated with commercial polymer-modified mortar and polymeric coatings," *Construction and Building Materials*, vol. 48, pp. 734–744, 2013, doi: 10.1016/j.conbuildmat.2013.07.099.
- [85] Y. Zhang and X. Kong, "Influences of superplasticizer, polymer latexes and asphalt emulsions on the pore structure and impermeability of hardened cementitious materials," *Construction and Building Materials*, vol. 53, pp. 392–402, 2014, doi: 10.1016/j.conbuildmat.2013.11.104.
- [86] E. Booya, K. Mermerdas, E. Güneyisi, and M. Gesog, "Strength and permeability properties of self-compacting concrete with cold bonded fly ash lightweight aggregate," *Construction and Building Materials*, vol. 74, pp. 17–24, 2015.
- [87] P. Duan, Z. Shui, W. Chen, and C. Shen, "Efficiency of mineral admixtures in concrete: Microstructure, compressive strength and stability of hydrate phases," *Applied Clay Science*, vol. 83–84, pp. 115–121, 2013, doi: 10.1016/j.clay.2013.08.021.
- [88] L. D. X. Y. & H. H. Sun Y., "Experimental study on mechanical properties and durability of recycled fine aggregate concrete in actual production.," *Build. Struct.*, 49, 81–84., 2019.
- [89] A. Mardani-Aghabaglou, M. Tuyan, and K. Ramyar, "Mechanical and durability performance of concrete incorporating fine recycled concrete and glass aggregates," *Materials and Structures/Materiaux et Constructions*, vol. 48, no. 8, pp. 2629–2640, 2015, doi: 10.1617/s11527-014-0342-3.
- [90] H. Sasanipour and F. Aslani, "Durability properties evaluation of self-compacting concrete prepared with waste fine and coarse recycled concrete aggregates," *Construction and Building Materials*, vol. 236, 2020, doi: 10.1016/j.conbuildmat.2019.117540.
- [91] K. Kapoor, S. P. Singh, and B. Singh, "Permeability of self-compacting concrete made with recycled concrete aggregates and metakaolin," *Journal of Sustainable Cement-Based Materials*, vol. 6, no. 5, pp. 293–313, 2017, doi: 10.1080/21650373.2017.1280426.
- [92] D. Mostofinejad, S. M. Hosseini, F. Nosouhian, T. Ozbakkaloglu, and B. Nader Tehrani, "Durability of concrete containing




- recycled concrete coarse and fine aggregates and milled waste glass in magnesium sulfate environment,” *Journal of Building Engineering*, vol. 29, 2020, doi: 10.1016/j.jobe.2020.101182.
- [93] T. Hemalatha and A. Ramaswamy, “A review on fly ash characteristics – Towards promoting high volume utilization in developing sustainable concrete,” *Journal of Cleaner Production*, vol. 147, pp. 546–559, 2017, doi: 10.1016/j.jclepro.2017.01.114.
- [94] P. Chindaprasirt, C. Jaturapitakkul, and T. Sinsiri, “Effect of fly ash fineness on microstructure of blended cement paste,” *Construction and Building Materials*, vol. 21, no. 7, pp. 1534–1541, 2007, doi: 10.1016/j.conbuildmat.2005.12.024.
- [95] M. H. Zhang, L. Li, and P. Paramasivam, “Shrinkage of high-strength lightweight aggregate concrete exposed to dry environment,” *ACI Materials Journal*, vol. 102, no. 2, pp. 86–92, 2005, doi: 10.14359/14301.
- [96] M. Gesoglu, E. Güneyisi, H. Ö. Öz, M. T. Yasemin, and I. Taha, “Durability and shrinkage characteristics of self-compacting concretes containing recycled coarse and/or fine aggregates,” *Advances in Materials Science and Engineering*, vol. 2015, 2015, doi: 10.1155/2015/278296.
- [97] D. Kong, T. Lei, J. Zheng, C. Ma, J. Jiang, and J. Jiang, “Effect and mechanism of surface-coating pozzalanics materials around aggregate on properties and ITZ microstructure of recycled aggregate concrete,” *Construction and Building Materials*, vol. 24, no. 5, pp. 701–708, 2010, doi: 10.1016/j.conbuildmat.2009.10.038.
- [98] V. W. Y. Tam, “Comparing the implementation of concrete recycling in the Australian and Japanese construction industries,” *Journal of Cleaner Production*, vol. 17, no. 7, pp. 688–702, 2009, doi: 10.1016/j.jclepro.2008.11.015.
- [99] W. Zhang, S. Wang, P. Zhao, L. Lu, and X. Cheng, “Effect of the optimized triple mixing method on the ITZ microstructure and performance of recycled aggregate concrete,” *Construction and Building Materials*, vol. 203, pp. 601–607, 2019, doi: 10.1016/j.conbuildmat.2019.01.071.
- [100] H. Mefteh, O. Kebaili, H. Oucief, L. Berredjem, and N. Arabi, “Influence of moisture conditioning of recycled aggregates on the properties of fresh and hardened concrete,” *Journal of Cleaner Production*, vol. 54, pp. 282–288, 2013, doi: 10.1016/j.jclepro.2013.05.009.
- [101] Y. Zhuang, Y. Liang, A. Nabizadeh, Z. Ng, T. Ji, and Y. F. Chen, “Influence of the moisture state of recycled fine aggregate on the impermeability of concrete,” *Materialprüfung/Materials Testing*, vol. 61, no. 10, pp. 991–998, 2019, doi: 10.3139/120.111412.
- [102] A. Ahmad, W. Ahmad, F. Aslam, and P. Joyklad, “Compressive strength prediction of fly ash-based geopolymer concrete via advanced machine learning techniques,” *Case Studies in Construction Materials*, vol. 16, 2022, doi: 10.1016/j.cscm.2021.e00840.
- [103] D. C. Feng *et al.*, “Machine learning-based compressive strength prediction for concrete: An adaptive boosting approach,” *Construction and Building Materials*, vol. 230, 2020, doi: 10.1016/j.conbuildmat.2019.117000.
- [104] A. Ahmad, K. Chaiyasarn, F. Farooq, W. Ahmad, S. Suparp, and F. Aslam, “Compressive strength prediction via gene expression programming (GEP) and artificial neural network (ANN) for concrete containing rca,” *Buildings*, vol. 11, no. 8, 2021, doi: 10.3390/buildings11080324.
- [105] J. Rahman, K. S. Ahmed, N. I. Khan, K. Islam, and S. Mangalathu, “Data-driven shear strength prediction of steel fiber reinforced concrete beams using machine learning approach,” *Engineering Structures*, vol. 233, 2021, doi: 10.1016/j.engstruct.2020.111743.
- [106] S. Z. Chen, S. Y. Zhang, W. S. Han, and G. Wu, “Ensemble learning based approach for FRP-concrete bond strength prediction,” *Construction and Building Materials*, vol. 302, 2021, doi: 10.1016/j.conbuildmat.2021.124230.
- [107] X. Wang, Y. Liu, and H. Xin, “Bond strength prediction of concrete-encased steel structures using hybrid machine learning method,” *Structures*, vol. 32, pp. 2279–2292, 2021, doi: 10.1016/j.istruc.2021.04.018.
- [108] M. Ahmad *et al.*, “Supervised learning methods for modeling concrete compressive strength prediction at high temperature,” *Materials*, vol. 14, no. 8, 2021, doi: 10.3390/ma14081983.
- [109] D. Van Dao *et al.*, “A sensitivity and robustness analysis of GPR and ANN for high-performance concrete compressive strength prediction using a monte carlo simulation,” *Sustainability (Switzerland)*, vol. 12, no. 3, 2020, doi: 10.3390/su12030830.
- [110] M. A. DeRousseau, E. Laftchiev, J. R. Kasprzyk, B. Rajagopalan, and W. V. Srubar, “A comparison of machine learning methods for predicting the compressive strength of field-placed concrete,” *Construction and Building Materials*, vol. 228, 2019, doi: 10.1016/j.conbuildmat.2019.08.042.
- [111] M. N. Amin, M. Iqbal, K. Khan, M. G. Qadir, F. I. Shalabi, and A. Jamal, “Ensemble tree-based approach towards flexural strength prediction of FRP reinforced concrete beams,” *Polymers*, vol. 14, no. 7, 2022, doi: 10.3390/polym14071303.
- [112] H. Song *et al.*, “Predicting the compressive strength of concrete with fly ash admixture using machine learning algorithms,” *Construction and Building Materials*, vol. 308, 2021, doi: 10.1016/j.conbuildmat.2021.125021.
- [113] Z. Wan, Y. Xu, and B. Šavija, “On the use of machine learning models for prediction of compressive strength of concrete: Influence of dimensionality reduction on the model performance,” *Materials*, vol. 14, no. 4, pp. 1–23, 2021, doi: 10.3390/ma14040713.
- [114] T. Oey, S. Jones, J. W. Bullard, and G. Sant, “Machine learning can predict setting behavior and strength evolution of hydrating cement systems,” *Journal of the American Ceramic Society*, vol. 103, no. 1, pp. 480–490, 2020, doi: 10.1111/jace.16706.
- [115] A. Ahmad *et al.*, “Prediction of geopolymer concrete compressive strength using novel machine learning algorithms,” *Polymers*, vol. 13, no. 19, 2021, doi: 10.3390/polym13193389.

## BIOGRAPHIES OF AUTHORS



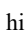


**Esra'a Alhenawi**    She is a dedicated academic with a distinguished background in computer science. She earned her Ph.D. in computer science with honors in 2022, following her master's degree in the same field in 2015. She also holds a bachelor's degree in computer engineering from 2010, currently serving as an assistant professor at Zarqa University since September 2023. She can be contacted at email: ealhenawi@zu.edu.jo.






**Ayat Mahmoud Al-Hinawi**    received her Bs degree in civil engineering in 2008 from Jordan university of science and technology, in 2013 received her master's degree in structural engineering from Jordan University of science and technology. Currently she works as a lecturer at Hashimate University. She has researched structural engineering and artificial intelligence. She can be contacted at email: [ayat05@hu.edu.jo](mailto:ayat05@hu.edu.jo)



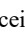


**Zaher Salah**    received his Ph.D. degree in computer science from the University of Liverpool, UK, in 2014, his MSc degree in computer science from Yarmouk University, Jordan, in 2004, and his B.Sc. degree in computer science from University of Jordan, Jordan, in 2001. He is currently an Associate Professor in the Information Technology Department of the Hashemite University, Zarqa, Jordan. His research interests include machine learning, cyber security, information retrieval, opinion mining, sentiment analysis, biometrics, digital image and analysis, and pattern recognition. He can be contacted at email: [zaher@hu.edu.jo](mailto:zaher@hu.edu.jo).



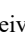


**Omar Khair Alla Alidmat**    received his B.Sc. degree in computer information systems, M.Sc. degree in computer science from Al al-Bayt University, Jordan, and the Ph.D. degree in computer science from Universiti Sains Malaysia, Malaysia. Currently, Dr. Alidmat serves as an assistant professor in the Computer Science Department at Zarqa University, Jordan. His Ph.D. research focused on artificial intelligence, specializing in modelling crowd movements in panic situations, such as fires. He can be contacted at: [oalidmat@zu.edu.jo](mailto:oalidmat@zu.edu.jo).






**Esraa Abu Elsoud**    received the B.Sc. degree in electrical engineering from The Hashemite University, Jordan, in 2013 and M.Sc. in Cyber Security from The Hashemite University in 2023. Eng. Esraa's current research interests include cyber security, machine learning, big data and mobile network. She is currently a Lecturer in Zarqa University, Zarqa, Jordan. She can be contacted at email: [eabuelsoud@zu.edu.jo](mailto:eabuelsoud@zu.edu.jo).



**Raed Alazaidah**    received the B.Sc. degrees in computer information system, M.Sc. degrees in computer science from AL al-Bayt University, Jordan, in 2012 and 2015, respectively, and the Ph.D. degree in Computer Science from University Sains Malaysia, Malaysia, in 2023. He can be contacted at email: [razaidah@zu.edu.jo](mailto:razaidah@zu.edu.jo).



**Bashar Rizik AlSayed**    graduated from the University of Jordan in 2020 with a B.Sc. in civil engineering. He is presently enrolled in the University of Jordan's School of Engineering to pursue an M.Sc. in transportation, with a fall 2024 graduation date anticipated. Eng. Bashar completed a project for his bachelor's degree called "Time and Cost Management for a Residential Building in Jordan" that was deemed exceptional. For over three years, Eng. Bashar was employed as a site engineer. Engineer Bashar is quite proficient in AutoCAD, Primavera, C++, Microsoft Project, and Microsoft Office (Word, Excel, Access, PowerPoint). He can be contacted at email: [basharalsayed1996@gmail.com](mailto:basharalsayed1996@gmail.com).